

Preparation and evaluation of novel bamboo-polymer composites

L. Bhowmik and J. K. Ray*

Department of Chemistry, Indian Institute of Technology,
Kharagpur 721302, India

Abstract. Monomer impregnated bamboo fibres were polymerized by radically initiated polymerization technique to prepare novel composite materials. These composites exhibit close to a linear elastic behaviour. Scanning electron microscopic studies of these composites reveal a uniform incorporation of polymer into bamboo fibre matrix. These composites are also thermally stable. In view of the very low cost and ease of processing and manufacturing associated with bamboo-polymer composites, it is revealed that they offer an attractive possibility for exploitation as commercially viable biocompatible material for various structural applications.

Keywords. Composites, polymer impregnated, radical initiator, thermal stability.

* Corresponding author

1. Introduction

Fibre reinforced composite materials using synthetic resins have achieved significant development in the last few decades because of their desirable properties such as light weight, high strength to weight ratio and comparatively easy processability. Most commercially important composites are based on glass fibre as the reinforcing material. Other fibres that have been successfully utilized for composite preparation include carbon, boron, asbestos fibres etc¹⁻⁵. Sophisticated preparation techniques and high production cost limited the use of synthetic fibres like aramid, glass, carbon, silica, alumina, silicon carbide etc. Of late, cellulose has been used as a substitute for synthetic fibre especially for polymer matrix composites. Among known natural fibres, jute, coir, sisal, ramie, banana fibre have relatively low or poor mechanical strength⁶⁻⁹. Bamboo is one of the fastest growing plants and is abundantly available in most countries. However, work reported to date on bamboo fibre reinforced composite is very limited and a thorough study is warranted in view of its unique structure, vis-à-vis many attractive bulk properties of its composites¹⁰⁻¹³. There has also been a rising trend in the use of polymers and polymer composites and macromolecules mostly from bio-available sources for a host of applications encompassing medical diagnosis, therapy, agriculture and sustainable building materials^{2, 4, 8, 14-40}.

Bamboo, a natural ligno-cellulosic composite, is attracting more attention of scientists and engineers owing to its unique biological structure. Plants on the earth develop their structure to adapt to various environments over a long period of time. Bamboo may be a typical example of plant with highly developed architecture. The geometry of bamboo longitudinal profile has a microscopically functional graded structure that helps it to withstand extreme natural environment^{41, 42} and it is a unique example of unidirectional fiber reinforced composite. It has been observed that the fibre distribution in the cross section at any particular height is dense in the outer region and spares in the inner surface. As a result, the outer portion exhibits a higher strength than the inner core. The fibre strength is 600 MPa, which is 12 times higher than the matrix strength and the corresponding Young's modulus of the fiber is also much larger than that of the matrix. In addition to these investigations, the use of bamboo as a structural material as much as a reinforcement of composite material is also wide and competitive. Several attempts have been made in the past to study the mechanical properties such as modulus and strength of bamboo and bamboo composite^{1, 10, 41, 42}. These studies include testing of whole bamboo as well

sections, strips and fibres of bamboo. Amada et al. examined the structure variation in bamboo with cross section and height⁴¹. The fraction of cellulosic fibre varied from 15-20 % to 60-65%. Tensile strength and modulus varied from 100 to 600 MPa and 3 to 15 GPa, respectively. Jain et al. reported the anatomical properties of bamboo and bamboo fibre reinforced plastic with different orientations. They evaluated tensile, flexural and impact strength of bamboo and bamboo fiber reinforced plastic composite with different orientations⁴³. Shin and coworkers fabricated and tested bamboo strips and epoxy resin composite⁴⁴. They observed that the epoxy resin composite is superior in strength to that of glass-fibre reinforced epoxy resin and have greater durability.

In our work we have tried to remove either full or partial matrix part of bamboo keeping the overall structure of bamboo undisturbed. Our main aim was to develop a durable and higher strength bamboo polymer composite having structurally stronger polymer components.

2. Experimental

2.1 Materials

Bamboo (B) specimens used in the present investigation *viz.* Valqua were collected from southern part of West Bengal, India. The bamboo specimen was air dried for 30 days in the open atmosphere.

Methyl methacrylate (MMA), methyl acrylate (MA) and styrene (S) were purchased from Qualigens, India. The monomers were purified with 5% sodium hydroxide solution followed by washing with distilled water. Finally, the washed monomer was dried over fused calcium chloride and distilled under vacuum. Phenol (AR) (E. Merck, India) was used after distillation. Formaldehyde (Qualigens, India) and NaOH (G.R) (E. Merck, India) were used as received.

2.2 Preparation and conditioning of bamboo specimen

For polymer impregnation in bamboo strips, dumbbell shaped specimens were used keeping in view the measurement of mechanical properties of the bamboo-polymer composites. Tensile specimens were treated with 15% NaOH solution to partially remove the matrix as reported in literature⁴⁵. This parameter was chosen to optimize matrix removal keeping the overall structure

of bamboo undisturbed. Alkali treatment changed the colour of the bamboo fibre from brown to pale yellow. The samples were then thoroughly washed with distilled water to ensure complete removal of alkali and subsequently dried in an oven at 60 °C for overnight.

Alkali treated bamboo specimens were soaked with different monomers, *viz.* MMA, MA, S at 25 °C for 2 h. *In situ* polymerization of these monomers within the bamboo specimen was carried out in a specially designed reaction vessel fitted with inlet and outlet system for deaeration. For soaking with different monomers, the alkali treated specimens were separately immersed within the vessel in 40% benzene solution of MA, MMA and S containing 0.1% benzoyl peroxide as initiator in each case. The contents in the reaction vessel were deaerated by passing dry N₂ for 1 h. The polymerization of the respective monomer soaked within the bamboo matrix was carried out by placing the vessel in a constant temperature bath at 70 °C for about 4 h. After polymerization, the specimens were removed from the vessel. The outer surface of the composite washed with solvent to remove the adhered polymer and dried in a vacuum oven at 60 °C to remove the unconverted monomer and benzene.

For *in situ* formation of phenol-formaldehyde resin within the bamboo specimen, the 15% alkali treated bamboo specimens were heated in aqueous solution of phenol and formaldehyde (1:1.2 mol) in presence of sodium hydroxide catalyst at 95-100 °C for 2 h. The phenolic resin (resol) soaked bamboo specimens were cured at 150 °C for 10 min in an oven. The percentage of different polymer loading within the bamboo specimen, measured gravimetrically, was calculated using the following equation:

$$\% \text{ Polymer loading} = \frac{X-Y}{Y} \times 100$$

Where, X is the weight of the bamboo specimen plus polymer formed and Y is the weight of the original bamboo specimen.

2.3 Characterization and Techniques

In order to measure the water absorption behaviour, the raw bamboo and bamboo-polymeric composites were cut into small pieces. These cut specimens were finely filed to remove any flaws. Before testing, the specimens were dried in an oven at 50 °C for 2 h and kept over fused

CaCl₂ for 24 h followed by weighing to record the initial weight (W_1). Then these samples were immersed in distilled water for 72 h at room temperature, taken out and wiped well with filter paper. The swelled weight (W_2) was measured again carefully and water absorption was calculated using the following equation:

$$\% \text{ Water absorption} = \frac{W_2 - W_1}{W_1} \times 100$$

Finely ground bamboo-polymer composite powder was used for FTIR analysis in KBr pellet by Thermo Nicolet FTIR Spectrophotometer (Model Nexus 870).

Tensile properties of virgin untreated bamboo specimens, alkali treated bamboo specimens, and bamboo polymer composite specimen were measured by using a universal testing machine (according to ASTM D-638-82) The dumbbell shaped specimens had a gauge length of 5 mm. A crosshead separation speed of 10 mm/min was used. Five specimens of each sample were tested. Specimens under tensile test were loaded until fracture developed.

Thermal analysis of bamboo-polymer composites was performed on a Shimadzu DT-40 unit, under N₂ atmosphere at a heating rate of 10 °C min⁻¹. The analyses were performed from room temperature to 900 °C.

Fracture surface morphology of the bamboo-polymer composite specimen was studied by a scanning electron microscope (Cam Scan 2DV unit) with various magnifications.

3. Results and discussion

The compositions of the bamboo-polymer composites as well as the composite specimen designations are shown in Table 1. In this investigation only the polymer impregnation within the bamboo matrix was desired, ignoring whether it occurred by grafting or homopolymerization. It is seen from Table 1 that maximum polymer loading within the bamboo matrix occurred in the cases of PMMA and phenolic resin in the same period of polymer formation. It was also interestingly observed that polymerization of styrene and acrylic monomers in bulk provided higher polymer loading than that in benzene solution.

During solution polymerization concentration of polymer was low, for this reason low incorporation of polymer took place. The main reason behind this observation was their different rates of conversion to polymers.

Table 1. Composition of bamboo-polymer composites.

Designation of composite	Polymer matrix	Polymerization medium	% Polymer loading	Density (g/cm ³)
B-PMMA (bul.)	Poly(methyl methacrylate)	--	24.4	1.21
B-PMA (bul.)	Poly(methyl acrylate)	--	14.4	1.16
B-PS (bul.)	Poly (styrene)	--	12.6	1.12
B-PMMA (sol.)	Poly(methyl methacrylate)	Benzene	8.5	1.11
B-PMA (sol.)	Poly(methyl acrylate)	Benzene	5.1	1.09
B-PS (sol.)	Poly(styrene)	Benzene	7.7	1.10
B-PF	Phenol-formaldehyde	Water *	24.4	1.19
Virgin bamboo	--	--	--	0.70

3.2 IR analysis

In order to assess physical entrapment and chemical attachment of the polymer molecules, if any, to the bamboo matrix, FTIR analysis of the composite specimens was done. FTIR spectrum of pure bamboo is shown in Figure. 1. Assignments of important IR bands are given in Table 2. The bands match well with the literature value.

Table 2. Characteristic infrared absorption bands of the bamboo and bamboo-polymer composites.

Characteristic band	Wave Number (cm ⁻¹)				
	Virgin B	B-PMMA	B-PMA	B-PS	B-PF
O-H str band (bonded)	3444	3440	3446.51	3420.43	3403.14
C-H str. band of CH ₃ or CH ₂	2919	2923	2861.03	2933.27	2901.07
O-CH ₃ str.	--	2851	--	--	--
C-H str. of aldehyde	--	2645	--	--	--
C=O (H-bonded)	--	1634.60	1615.49	1626.31	1619.21
Aromatic moiety of lignin	1432-1227	1449-1262	1460-1284	1435-1216	1414-1208
Skeletal vibration of cellulose and hemicellulose					

In every spectrum there was an intense broad band near about 3440 cm^{-1} for O-H stretching and hydrogen bonded O-H stretching of bamboo matrix, bamboo-polymer composite and also some moisture present in bamboo. Sharp peaks in the region 2919 cm^{-1} - 2923 cm^{-1} appeared due to C-H stretching of methyl and methylene groups present in both bamboo and bamboo- polymer composites. Few sharp and weak peaks in the region of 1269 – 1426 cm^{-1} in all bamboo and bamboo-polymer composites are designated to the skeletal vibration of cellulose, hemicellulose and lignin aromatic moiety. However, the appearance of peaks at 2851 cm^{-1} and 1384 cm^{-1} in the spectra of B-PMMA composite indicated the presence of O-CH₃ and C-H symmetric deformation of CH₃ group of PMMA. Moreover, the presence of a sharp peak at 2654 cm^{-1} was characteristic of the C-H stretching vibration of aldehyde group, which may be generated during grafting of PMMA to cellulose moiety of bamboo specimen.

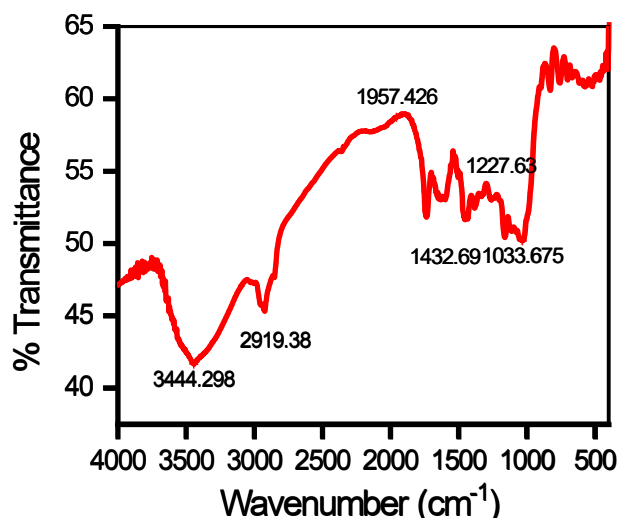


Figure 1. IR spectrum of bamboo.

3.2 SEM analysis

Fracture surface morphology of the bamboo-polymer composite specimens is shown in Figure. 2. Micro structural studies of the virgin bamboo (Figure. 2a) revealed many voids in the inner part of the bamboo. The fracture of fibre shows that each fiber, irrespective of its position, contained many fibrils. The cross section of fibrils appeared as hexagonal honeycombs bonded with each other. Again, fibril contains much continuously elongated cellulose in twisted forms. Overall bamboo fibre contains many fibrils, composed of cellulose. Figure 2b represents microstructure of alkali leached bamboo specimen where porosity was more than the virgin specimen due to the removal of some soluble sugars and hemicellulose. Figure 2c-2e represent the SEM micrographs of bamboo-poly (methyl methacrylate), bamboo-poly (methylacrylate) and bamboo-phenolic resin composites respectively. From the micrographs it was clear that polymers were evenly impregnated making a good bond with bamboo. Polymer impregnation into the bamboo matrix was also evinced from the higher density of the bamboo-polymer composites than that of the virgin bamboo.

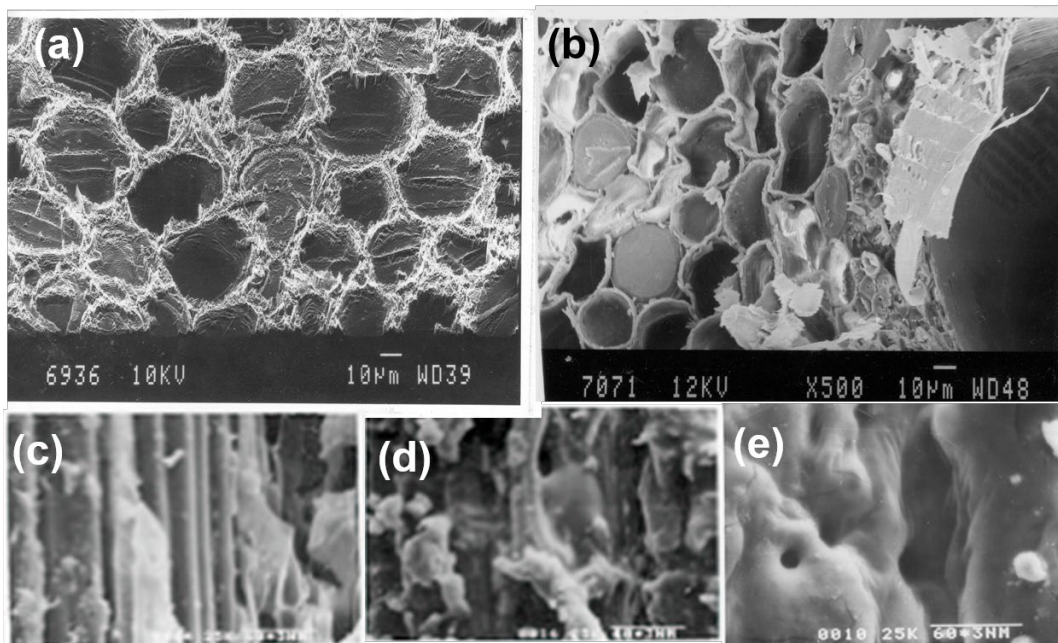


Figure. 2 SEM micrograph of **(a)** raw bamboo **(b)** alkali treated bamboo **(c)** Bamboo-PMMA **(d)** Bamboo-PMA **(e)** Bamboo-PF

3.3 Tensile strength analysis

One of the most important characteristics of these composites is their mechanical property. The values of tensile strength, elongation and modulus are given in Table 3.

Table 3. Mechanical properties of bamboo-polymer composites.

Sample Designation	Strain (mm/mm)	Modulus (GPa)	Tensile Strength (MPa)	Toughness (Joule)	Elongation at Break (%)
B-PMMA (bul)	0.059	13.468	356.83	5.07	5.93
B-PMA (bul)	0.034	11.713	272.43	2.15	3.43
B-PS (bul)	0.034	13.468	255.32	2.53	3.37
B-PMMA (sol)	0.030	8.228	224.49	--	3.00
B-PMA (sol)	0.018	13.179	197.54	0.48	1.84
B-PS (sol)	0.066	9.045	279.20	11.40	6.60
B-PF	0.038	9.335	289.63	1.396	3.83
Virgin bamboo	0.028	8.492	180.42	--	2.83
Alkali treated bamboo	0.020	5.717	102.17	0.68	1.97

The specimen under tensile test was loaded until fracture. Tensile load increased linearly with increasing strain until the point of ultimate load. Partial damage occurred in some specimens when the tensile load reached about 90% of the ultimate stress. The ultimate load carried by the set of fibers and ultimate extensions before failure were measured. To measure the elongation, two marks were made on the load axis and the change in the distance between the two marks were recorded for different loading conditions. Tensile strength was calculated from the ultimate load and cross-sectional area of fibers. Typical stress-strain curve of virgin bamboo is given in Figure 3. It showed a uniform increase in stress with strain followed by immediate fracture at the maximum load. Below 60 to 65% of breaking load, a linear relationship was recorded in the load displacement curve. Shin *et al.* reported the slippage prior breaking in this range for bamboo-epoxy composites⁴⁴. Similar trends were also observed in all the composites prepared using the

above-mentioned method. Using the stress strain curve, the tensile strength of alkali-leached bamboo specimen was calculated to be 102 MPa. The lower tensile strength of alkali treated bamboo specimen as compared to raw bamboo could be a reflection of poor bonding between fiber and matrix which promoted fracture. This may be due to the partial removal of matrix of bamboo during alkali treatment. Generally, fibers reinforce the matrix when the fiber and matrix are sufficient to restrain the stress distribution. Strength of a composite can achieve optimum levels when it has perfect interfacial adhesion and interfacial strength. From Table 3 it was observed that the tensile strength of B-PMMA and B-PS composites (prepared by bulk polymerization) was 356.83 MPa and 255.32 MPa respectively. Improved tensile properties of all the above-mentioned composites were due to stronger bonding between matrices or more incorporation of polymer into bamboo matrix. The overall stress-strain behavior of all bamboo polymer composites was non-linear. On the other hand, tensile strength of bamboo polymer composite of B-PMMA, B-PS, (prepared by solution polymerization condition) (given in Table 3) was 224.49 MPa, and 279.20 MPa respectively. Low tensile strength of the composite may be due to insufficient interfacial bonding or inadequate incorporation of polymer and interfacial bonding or inadequate incorporation of polymer between fiber and matrix plays a vital role in governing the mechanical properties of bamboo. During solution polymerization concentration of polymer was low, which might be a reason for low incorporation of polymer. This may be due to the fact that at low polymer loading the fiber matrix interface becomes weak. The decrease in tensile strength at low polymer loading could be a reflection of poor fiber adhesion between fiber and matrix, which promoted micro crack formation at the interface. Generally, a fiber starts reinforcing the matrix when fibers are sufficient to restrain the matrix leading to uniform stress distribution. The stress-strain curve of bamboo polymer composite predicts general linear elastic behavior of bamboo polymer composite. Tensile load increased linearly with increasing strain until the point of ultimate load, when bamboo fiber underwent breakage exhibiting brittle fracture.

It was observed that bamboo polymer composites had higher strength than that of raw bamboo. The load extension curve obtained during measurement of tensile properties of the B-PMMA composite specimen is shown in Figure 3. The general trend of the graph shows a linear increase prior to breaking load. Elongation of bamboo-polymer composites occurs in the range 1.84 to 6.03 %. The stress strain curves thus obtained show a uniform increase in strain with

increasing stress followed by immediate fracture at a maximum load. From the graph it is observed that the behavior of these composite is close to linear elastic and breaking load caused brittle fracture to occur. The modulus of elasticity was relatively low for bamboo and alkali treated bamboo polymer composite and produced large deformation. Swelling and shrinkage occurred due to absorption or release of water respectively. The shrinkage was high for immature bamboo and decreased with maturity. Due to the presence of hydroxyl and other polar groups in various constituents of bamboo matrix moisture regain was high. Ultimate tensile strength of B-PF composites was 289.63 MPa. The mechanical properties of the grafted or polymer loaded fiber were obtained from tensile tests as a function of the amount of grafted or loaded polymer. This indicates greater bonding between bamboo–matrix and polymer because of the presence of greater number of reactive groups.

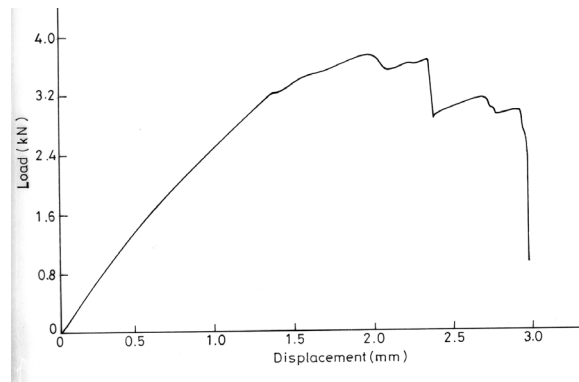


Figure.3 Load extension curve of PMMA-B Composite

The results showed substantial incorporation of polymer in the fiber matrix, which significantly improved the mechanical properties.

3.3 Water absorption behaviour

The degree of deterioration and reversibility of properties of the composite materials are largely dependent on the extent of moisture sorption. Natural fiber readily absorbs moisture because they contain abundant polar hydroxide groups, which results in a high moisture absorption level of

natural fiber reinforced polymer matrix composite and is a major obstacle for extensive application of natural fiber.

The sorption behavior of bamboo and bamboo polymer composites at 25 °C are given in Figure 4. It was clear from the graph that bamboo-polymer composites attributed lower moisture uptake than virgin bamboo. Water diffuses through the composite sample mainly by two possible mechanisms.

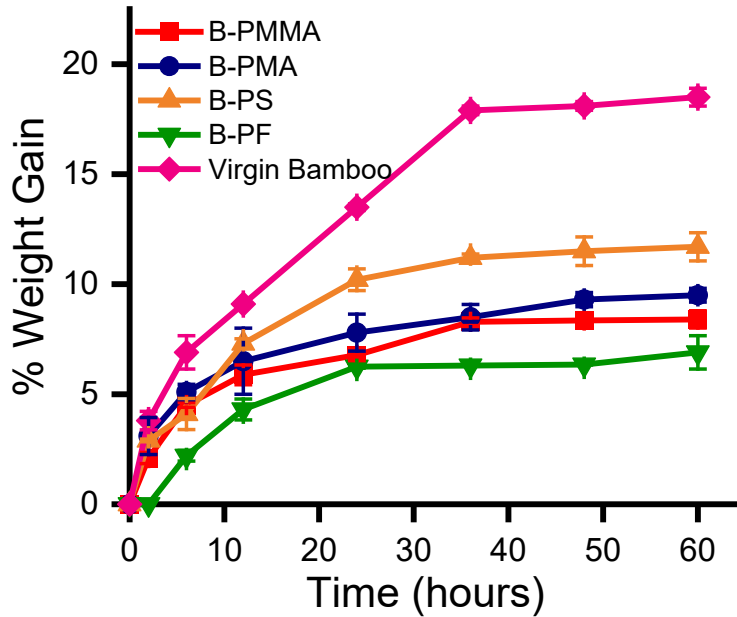


Figure 4. Water absorption characteristics of bamboo and bamboo-polymer composites

Water molecules diffuse directly into the matrix and reach the fibers or they enter into composite by capillary action along the fiber matrix interface followed by diffusion from the interface into bulk resin. The rate of water diffusion depends on the external conditions such as temperature, applied stress as well as internal material states such as debonding at fiber matrix interface, matrix cracking and inherent sorption property of constituent materials. The reduction in moisture level in the composite was attributed to an improved fiber/matrix interfacial bonding that reduces water accumulation in the interfacial voids and prevents water from entering the bamboo fiber. Due to the presence of hydroxyl and other polar groups in the various constituents of bamboo fibers the moisture regain was high which leads to poor wettability with resin and weak interfacial bonding between fibers and relatively more hygroscopic matrices. Future

research will be based on the measurement of mechanical strength and related properties of the bamboo-polymer composites after soaking of water.

3.4 Thermal analysis

Thermo gravimetric analysis was performed to evaluate the thermal stability of bamboo polymer composites. Prior to the thermo gravimetric analysis samples were left in air for 20 days.

Table 4. TGA analysis of bamboo and bamboo-polymer composites.

Sample designation	Decomposition temperature ($^{\circ}\text{C}$)											
	First stage				Second stage				Third stage			
	Initial	Peak	Final	% Wt Loss	Initial	Peak	Final	% Wt Loss	Initial	Peak	Final	% Wt Loss
B	22	80	90	17	90	265	387	54	387	395	997	20
PMMA	24	132	132	9	132	270	409	80	409	513	997	11
PMMA-B	19	100	112	5	112	395	482	60	482	510	1010	15
PF-B	22	125	197	12	197	420	532	37	532	560	987	25

Details of thermal degradation patterns of the virgin bamboo and bamboo-polymer composites are obtained from the TGA curves and included in Table 4. TGA curves of virgin bamboo, PMMA, B-PMMA composites, B-PF composites are given in Figure. 5a-5d. TGA curve of virgin bamboo has shown three distinct stages of degradation. Initial stage corresponds to a small loss in weight due to evaporation of absorbed moisture and it occurred nearly at 22-90 $^{\circ}\text{C}$. The second stage was associated with a sharp loss in weight (54%). Third stage of decomposition starts at 387 $^{\circ}\text{C}$. In both B-PMMA and B-PF composites, the first stage of decomposition occurred nearly at 19-112 $^{\circ}\text{C}$ and 22-197 $^{\circ}\text{C}$ respectively. In case of B-PMMA composite maximum weight loss occurred during the second stage degradation (60%). But in case of B-PF composite, comparable mass occurred in the second and third stages of decomposition. It was also observed that middle zone decomposition temperatures of both B-PMMA, B-PF composites were higher (340 $^{\circ}\text{C}$, 420 $^{\circ}\text{C}$) than those of bamboo (265 $^{\circ}\text{C}$), PMMA (270 $^{\circ}\text{C}$). Total weight losses are much less in case of the composite. From TGA analysis it may be concluded that the thermal stability of bamboo polymer composites have been improved after polymerization. However

experimental results at present level don't warrant a detailed explanation. More explanation on the thermal stability of the bamboo polymer composites needs further investigation.

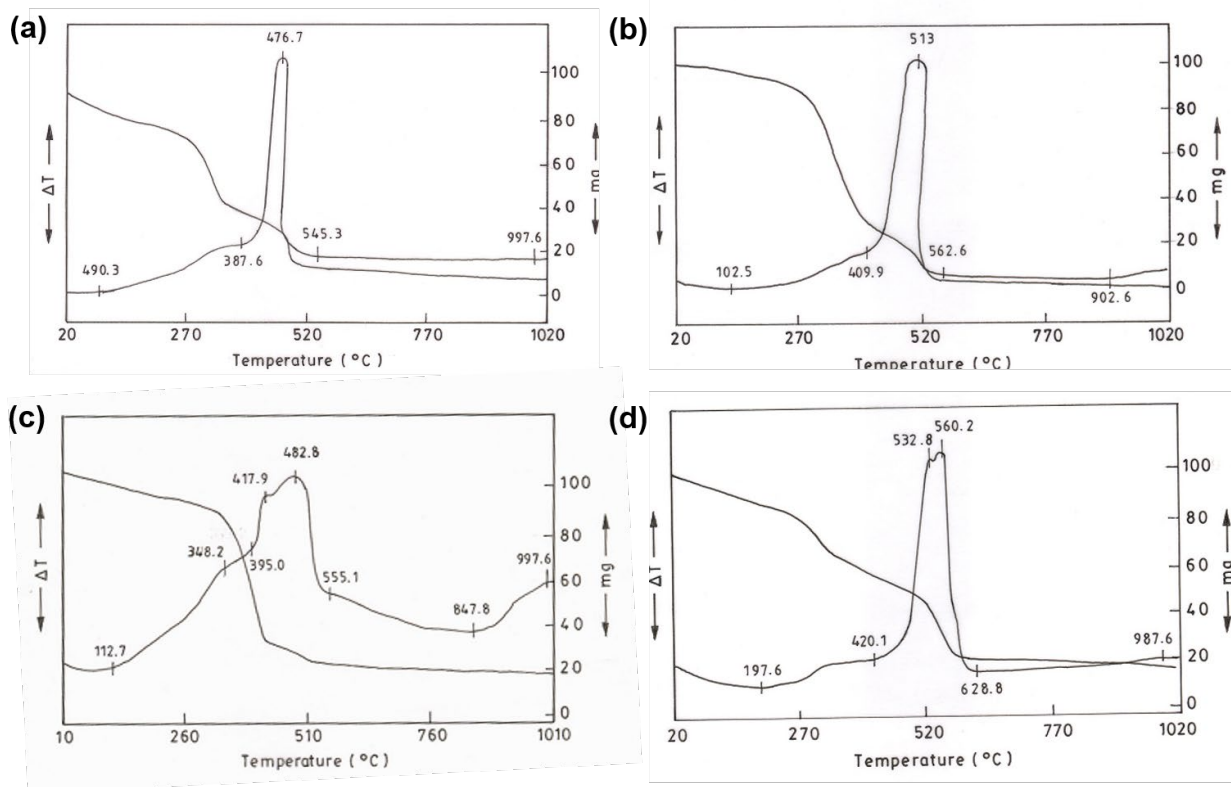


Figure. 5 Thermal gravimetric curves of (a) virgin bamboo (b) PMMA (c) PMMA-B composite (d) PF-B composite.

3.5 Durability study in boiling tetrahydrofuran (THF) and dimethyl formamide (DMF)

Durability of the above-mentioned polymer composites (after curing) was measured by measuring the weight loss after refluxing in THF and DMF for 24 h and 72 h. The data are presented in Table 5. The results showed that bamboo polymer composites exhibited slightly higher weight loss in DMF compared to that in THF. The higher weight loss in DMF was due to the prolonged heating at 150 $^{\circ}\text{C}$. B-PF composites showed almost negligible weight loss in both the solvents and this may be due to higher degree of cross-linking.

Table 5 Weight loss post in boiling tetrahydrofuran and dimethyl formamide

Leachant	Sample designation	% weight loss after refluxing	
		24h	72 h
THF	B-PMMA	1.32	1.71
	B-PMA	1.71	1.92
	B-ST	1.26	1.73
	B-PF	0.00	0.00
	B-PAN	2.14	3.40
	Virgin	2.16	3.29
DMF	B-PMMA	1.17	1.32
	B-PMA	1.72	2.51
	B-ST	1.56	2.18
	B-PF	1.12	2.01
	B-PAN	1.96	2.31
	Virgin	3.78	4.2

4. Conclusion

The above results have been demonstrated that a useful biocompatible composite material can be manufactured from bamboo fibre composite, and this can be regarded as a successful engineering material particularly lightweight building material with biocompatible and green properties.

Acknowledgement

The financial assistance received from Aeronautics Research and Development Board (ARDB), Govt. of India in carrying this investigation is gratefully acknowledged.

References

1. Ahmad, M.; Kamke, F. A., Analysis of Calcutta bamboo for structural composite materials: physical and mechanical properties. *Wood Science and Technology* **2005**, *39* (6), 448-459.
2. Ray, P.; Gidley, D.; Badding, J. V.; Lueking, A. D., UV and chemical modifications of polymer of Intrinsic Microporosity 1 to develop vibrational spectroscopic probes of surface chemistry and porosity. *Microporous and Mesoporous Materials* **2019**, *277*, 29-35.
3. Lager, J. R.; June, R. R., Compressive Strength of Boron-Epoxy Composites. *Journal of Composite Materials* **1969**, *3* (1), 48-56.
4. Ray, P.; Xu, E.; Crespi, V. H.; Badding, J. V.; Lueking, A. D., In situ vibrational spectroscopy of adsorbed nitrogen in porous carbon materials. *Physical Chemistry Chemical Physics* **2018**, *20* (22), 15411-15418.
5. Singh, T.; Rathi, M. K.; Patnaik, A.; Chauhan, R.; Ali, S.; Fekete, G., Application of waste tire rubber particles in non-asbestos organic brake friction composite materials. *Materials Research Express* **2018**, *6* (3), 035703.
6. Kulkarni, A. G.; Satyanarayana, K. G.; Rohatgi, P. K.; Vijayan, K., Mechanical properties of banana fibres (*Musa sapientum*). *Journal of Materials Science* **1983**, *18* (8), 2290-2296.
7. White, N. M.; Ansell, M. P., Straw-reinforced polyester composites. *Journal of Materials Science* **1983**, *18* (5), 1549-1556.
8. Sarker, N. C.; Ray, P.; Pfau, C.; Kalavacharla, V.; Hossain, K.; Quadir, M., Development of Functional Nanomaterials from Wheat Bran Derived Arabinoxylan for Nucleic Acid Delivery. *Journal of Agricultural and Food Chemistry* **2020**, *68* (15), 4367-4373.
9. Indra Reddy, M.; Anil Kumar, M.; Anki Reddy, S.; Vijaya Kumar Raju, P., Thermo physical properties of Jute, Pineapple leaf and Glass fiber reinforced polyester hybrid composites. *Materials Today: Proceedings* **2018**, *5* (10, Part 1), 21055-21060.
10. Sharma, B.; Gatóo, A.; Bock, M.; Ramage, M., Engineered bamboo for structural applications. *Construction and Building Materials* **2015**, *81*, 66-73.
11. Liese, W., Research on bamboo. *Wood Science and Technology* **1987**, *21* (3), 189-209.
12. Osorio, L.; Trujillo, E.; Van Vuure, A. W.; Verpoest, I., Morphological aspects and mechanical properties of single bamboo fibers and flexural characterization of bamboo/epoxy composites. *Journal of reinforced plastics and composites* **2011**, *30* (5), 396-408.
13. Okubo, K.; Fujii, T.; Yamamoto, Y., Development of bamboo-based polymer composites and their mechanical properties. *Composites Part A: Applied Science and Manufacturing* **2004**, *35* (3), 377-383.
14. Kunst, F.; Ogasawara, N.; Moszer, I.; Albertini, A. M.; Alloni, G.; Azevedo, V.; Bertero, M. G.; Bessières, P.; Bolotin, A.; Borchert, S.; Borriss, R.; Boursier, L.; Brans, A.; Braun, M.; Brignell, S. C.; Bron, S.; Brouillet, S.; Bruschi, C. V.; Caldwell, B.; Capuano, V.; Carter, N. M.; Choi, S. K.; Codani, J. J.; Connerton, I. F.; Cummings, N. J.; Daniel, R. A.; Denizot, F.; Devine, K. M.; Düsterhöft, A.; Ehrlich, S. D.; Emmerson, P. T.; Entian, K. D.; Errington, J.; Fabret, C.; Ferrari, E.; Foulger, D.; Fritz, C.; Fujita, M.; Fujita, Y.; Fuma, S.; Galizzi, A.; Galleron, N.; Ghim, S. Y.; Glaser, P.; Goffeau, A.; Golightly, E. J.; Grandi, G.;

- Guisseppi, G.; Guy, B. J.; Haga, K.; Haiech, J.; Harwood, C. R.; Hénaut, A.; Hilbert, H.; Holsappel, S.; Hosono, S.; Hullo, M. F.; Itaya, M.; Jones, L.; Joris, B.; Karamata, D.; Kasahara, Y.; Klaerr-Blanchard, M.; Klein, C.; Kobayashi, Y.; Koetter, P.; Koningstein, G.; Krogh, S.; Kumano, M.; Kurita, K.; Lapidus, A.; Lardinois, S.; Lauber, J.; Lazarevic, V.; Lee, S. M.; Levine, A.; Liu, H.; Masuda, S.; Mauël, C.; Médigue, C.; Medina, N.; Mellado, R. P.; Mizuno, M.; Moestl, D.; Nakai, S.; Noback, M.; Noone, D.; O'Reilly, M.; Ogawa, K.; Ogiwara, A.; Oudega, B.; Park, S. H.; Parro, V.; Pohl, T. M.; Portetelle, D.; Porwollik, S.; Prescott, A. M.; Presecan, E.; Pujic, P.; Purnelle, B.; Rapoport, G.; Rey, M.; Reynolds, S.; Rieger, M.; Rivolta, C.; Rocha, E.; Roche, B.; Rose, M.; Sadaie, Y.; Sato, T.; Scanlan, E.; Schleich, S.; Schroeter, R.; Scoffone, F.; Sekiguchi, J.; Sekowska, A.; Seror, S. J.; Serror, P.; Shin, B. S.; Soldo, B.; Sorokin, A.; Tacconi, E.; Takagi, T.; Takahashi, H.; Takemaru, K.; Takeuchi, M.; Tamakoshi, A.; Tanaka, T.; Terpstra, P.; Tognoni, A.; Tosato, V.; Uchiyama, S.; Vandebol, M.; Vannier, F.; Vassarotti, A.; Viari, A.; Wambutt, R.; Wedler, E.; Wedler, H.; Weitzenegger, T.; Winters, P.; Wipat, A.; Yamamoto, H.; Yamane, K.; Yasumoto, K.; Yata, K.; Yoshida, K.; Yoshikawa, H. F.; Zumstein, E.; Yoshikawa, H.; Danchin, A., The complete genome sequence of the Gram-positive bacterium *Bacillus subtilis*. *Nature* **1997**, *390* (6657), 249-256.
15. Ray, P.; Ferraro, M.; Haag, R.; Quadir, M., Dendritic Polyglycerol-Derived Nano-Architectures as Delivery Platforms of Gemcitabine for Pancreatic Cancer. *Macromol Biosci* **2019**, *19* (7), e1900073.
16. Plank, J., Applications of biopolymers and other biotechnological products in building materials. *Applied microbiology and biotechnology* **2004**, *66* (1), 1-9.
17. Ray, P.; Kale, N.; Quadir, M., New Side Chain Design for pH-Responsive Block Copolymers for Drug Delivery. *Colloids and Surfaces B: Biointerfaces* **2021**, 111563.
18. Abdullah, C. S.; Ray, P.; Alam, S.; Kale, N.; Aishwarya, R.; Morshed, M.; Dutta, D.; Hudziak, C.; Banerjee, S. K.; Mallik, S.; Banerjee, S.; Bhuiyan, M. S.; Quadir, M., Chemical Architecture of Block Copolymers Differentially Abrogate Cardiotoxicity and Maintain the Anticancer Efficacy of Doxorubicin. *Molecular Pharmaceutics* **2020**.
19. Ray, P.; Dutta, D.; Haque, I.; Nair, G.; Mohammed, J.; Parmer, M.; Kale, N.; Orr, M.; Jain, P.; Banerjee, S.; Reindl, K. M.; Mallik, S.; Kambhampati, S.; Banerjee, S. K.; Quadir, M., pH-Sensitive Nanodrug Carriers for Codelivery of ERK Inhibitor and Gemcitabine Enhance the Inhibition of Tumor Growth in Pancreatic Cancer. *Molecular Pharmaceutics* **2020**.
20. Trubetskoy, V. S., Polymeric micelles as carriers of diagnostic agents. *Advanced drug delivery reviews* **1999**, *37* (1-3), 81-88.
21. Ray, P.; Confeld, M.; Borowicz, P.; Wang, T.; Mallik, S.; Quadir, M., PEG-b-poly (carbonate)-derived nanocarrier platform with pH-responsive properties for pancreatic cancer combination therapy. *Colloids and Surfaces B: Biointerfaces* **2019**, *174*, 126-135.
22. Fleige, E.; Quadir, M. A.; Haag, R., Stimuli-responsive polymeric nanocarriers for the controlled transport of active compounds: concepts and applications. *Adv Drug Deliv Rev* **2012**, *64* (9), 866-84.
23. Krause, W., Delivery of diagnostic agents in computed tomography. *Advanced drug delivery reviews* **1999**, *37* (1-3), 159-173.
24. Ray, P.; Nair, G.; Ghosh, A.; Banerjee, S.; Golovko, M. Y.; Banerjee, S. K.; Reindl, K. M.; Mallik, S.; Quadir, M., Microenvironment-sensing, nanocarrier-mediated delivery of combination chemotherapy for pancreatic cancer. *Journal of Cell Communication and Signaling* **2019**.

25. Haag, R.; Kratz, F., Polymer Therapeutics: Concepts and Applications. *Angewandte Chemie International Edition* **2006**, *45* (8), 1198-1215.
26. Ray, P.; Alhalhooly, L.; Ghosh, A.; Choi, Y.; Banerjee, S.; Mallik, S.; Banerjee, S.; Quadir, M., Size-Transformable, Multifunctional Nanoparticles from Hyperbranched Polymers for Environment-Specific Therapeutic Delivery. *ACS Biomaterials Science & Engineering* **2019**, *5* (3), 1354-1365.
27. Clément, M.; Abdellah, I.; Ray, P.; Martini, C.; Coppel, Y.; Remita, H.; Lampre, I.; Huc, V., Synthesis and NMR study of trimethylphosphine gold(i)-appended calix[8]arenes as precursors of gold nanoparticles. *Inorganic Chemistry Frontiers* **2020**.
28. Ray, P.; Clément, M.; Martini, C.; Abdellah, I.; Beaunier, P.; Rodriguez-Lopez, J.-L.; Huc, V.; Remita, H.; Lampre, I., Stabilisation of small mono- and bimetallic gold-silver nanoparticles using calix[8]arene derivatives. *New Journal of Chemistry* **2018**, *42* (17), 14128-14137.
29. André, E.; Boutonnet, B.; Charles, P.; Martini, C.; Aguiar-Hualde, J.-M.; Latil, S.; Guérineau, V.; Hammad, K.; Ray, P.; Guillot, R.; Huc, V., A New, Simple and Versatile Strategy for the Synthesis of Short Segments of Zigzag-Type Carbon Nanotubes. *Chemistry – A European Journal* **2016**, *22* (9), 3105-3114.
30. Ray, P.; Gray, J. L.; Badding, J. V.; Lueking, A. D., High-Pressure Reactivity of Triptycene Probed by Raman Spectroscopy. *The Journal of Physical Chemistry B* **2016**, *120* (42), 11035-11042.
31. Chaudhuri, S.; Maity, S.; Roy, M.; Ray, P.; Ray, J. K., A Vinyl Radical Cyclization Route to Hydroxycyclohexene Fused Carbocycles. *Asian Journal of Chemistry* **2016**, *28* (1).
32. Ray, J. K.; Paul, S.; Ray, P.; Singha, R.; Rao, D. Y.; Nandi, S.; Anoop, A., Pd-catalyzed intramolecular sequential Heck cyclization and oxidation reactions: a facile pathway for the synthesis of substituted cycloheptenone evaluated using computational studies. *New Journal of Chemistry* **2017**, *41* (1), 278-284.
33. Ray, J. K.; Singha, R.; Ray, D.; Ray, P.; Rao, D. Y.; Anoop, A., Palladium-catalyzed expedient Heck annulations in 1-bromo-1,5-dien-3-ols: Exceptional formation of fused bicycles. *Tetrahedron Letters* **2019**, *60* (13), 931-935.
34. Ray, P., Interactions of nitrogen and hydrogen with various 1D and 3D carbon materials probed via in-situ vibrational spectroscopy. *Ph. D. Thesis* **2016**.
35. Wang, C.-Y.; Ray, P.; Gong, Q.; Zhao, Y.; Li, J.; Lueking, A. D., Influence of gas packing and orientation on FTIR activity for CO chemisorption to the Cu paddlewheel. *Physical Chemistry Chemical Physics* **2015**, *17* (40), 26766-26776.
36. Ray, P., Interactions of nitrogen and hydrogen with various 1D and 3D carbon materials probed via in-situ vibrational spectroscopy. **2016**.
37. Confeld, M. I.; Mamnoon, B.; Feng, L.; Jensen-Smith, H.; Ray, P.; Froberg, J.; Kim, J.; Hollingsworth, M. A.; Quadir, M.; Choi, Y.; Mallik, S., Targeting the tumor core: hypoxia-responsive nanoparticles for delivery of chemotherapy to pancreatic tumors. *Molecular Pharmaceutics* **2020**.
38. Ghosh, A.; Sarkar, S.; Ghosh, S.; Ray, P.; Quadir, M.; Banerjee, S. K.; Banerjee, S., Abstract 1234: Zoledronic acid-induced suppression of invasive phenotypes of pancreatic cancer cells is mediated through downregulation of CYR61/CCN1. *Cancer Research* **2019**, *79* (13 Supplement), 1234.
39. Das, A.; Haque, I.; Ray, P.; Ghosh, A.; Dutta, D.; Quadir, M.; De, A.; Gunewardena, S.; Chatterjee, I.; Banerjee, S.; Weir, S.; Banerjee, S. K., CCN5 activation by free or

encapsulated EGCG is required to render triple-negative breast cancer cell viability and tumor progression. *Pharmacol Res Perspect* **2021**, *9* (2), e00753.

40. Ray, P.; Haideri, N.; Haque, I.; Mohammed, O.; Chakraborty, S.; Banerjee, S.; Quadir, M.; Brinker, A. E.; Banerjee, S. K., The Impact of Nanoparticles on the Immune System: A Gray Zone of Nanomedicine. *Journal of Immunological Sciences* **2021**, *5* (1).

41. Amada, S.; Ichikawa, Y.; Munekata, T.; Nagase, Y.; Shimizu, H., Fiber texture and mechanical graded structure of bamboo. *Composites Part B: Engineering* **1997**, *28* (1), 13-20.

42. Jain, S.; Jindal, U. C.; Kumar, R., Development and fracture mechanism of the bamboo/polyester resin composite. *Journal of Materials Science Letters* **1993**, *12* (8), 558-560.

43. Jain, S.; Kumar, R.; Jindal, U. C., Mechanical behaviour of bamboo and bamboo composite. *Journal of Materials Science* **1992**, *27* (17), 4598-4604.

44. Shin, F. G.; Xian, X. J.; Zheng, W. P.; Yipp, M. W., Analyses of the mechanical properties and microstructure of bamboo-epoxy composites. *Journal of Materials Science* **1989**, *24* (10), 3483-3490.

45. Deshpande, A. P.; Bhaskar Rao, M.; Lakshmana Rao, C., Extraction of bamboo fibers and their use as reinforcement in polymeric composites. *Journal of Applied Polymer Science* **2000**, *76* (1), 83-92.